Comparison of GOME tropospheric NO2 columns with NO2 profiles deduced from ground-based in situ measurements

D. Schaub, K. F. Boersma, J. W. Kaiser, A. K. Weiss, D. Folini, H. J. Eskes, B. Buchmann

Atmos. Chem. Phys., 6, 3211–3229, 2006
www.atmos-chem-phys.net/6/3211/2006/

Atmospheric Chemistry and Physics

Comparison of GOME tropospheric NO_2 columns with NO_2 profiles deduced from ground-based in situ measurements

D. Schaub[1], **K. F. Boersma**[2], **J. W. Kaiser**[3], **A. K. Weiss**[1], **D. Folini**[1], **H. J. Eskes**[2], **and B. Buchmann**[1]

[1]Empa, Swiss Federal Laboratories for Materials Testing and Research, Ueberlandstrasse 129, CH-8600 Duebendorf, Switzerland
[2]Royal Netherlands Meteorological Institute (KNMI), P.O. Box 201, 3730 AE, De Bilt, The Netherlands
[3]European Centre for Medium-Range Weather Forecasts (ECMWF), Shinfield Park, Reading, RG2 9AX, UK

Received: 10 January 2006 – Published in Atmos. Chem. Phys. Discuss.: 31 March 2006
Revised: 23 June 2006 – Accepted: 28 July 2006 – Published: 3 August 2006

Abstract. Nitrogen dioxide (NO_2) vertical tropospheric column densities (VTCs) retrieved from the Global Ozone Monitoring Experiment (GOME) are compared to coincident ground-based tropospheric NO_2 columns. The ground-based columns are deduced from in situ measurements at different altitudes in the Alps for 1997 to June 2003, yielding a unique long-term comparison of GOME NO_2 VTC data retrieved by a collaboration of KNMI (Royal Netherlands Meteorological Institute) and BIRA/IASB (Belgian Institute for Space Aeronomy) with independently derived tropospheric NO_2 profiles. A first comparison relates the GOME retrieved tropospheric columns to the tropospheric columns obtained by integrating the ground-based NO_2 measurements. For a second comparison, the tropospheric profiles constructed from the ground-based measurements are first multiplied with the averaging kernel (AK) of the GOME retrieval. The second approach makes the comparison independent from the a priori NO_2 profile used in the GOME retrieval. This allows splitting the total difference between the column data sets into two contributions: one that is due to differences between the a priori and the ground-based NO_2 profile shapes, and another that can be attributed to uncertainties in both the remaining retrieval parameters (such as, e.g., surface albedo or aerosol concentration) and the ground-based in situ NO_2 profiles. For anticyclonic clear sky conditions the comparison indicates a good agreement between the columns (n=157, R=0.70/0.74 for the first/second comparison approach, respectively). The mean relative difference (with respect to the ground-based columns) is -7% with a standard deviation of 40% and GOME on average slightly underestimating the ground-based columns. Both data sets show a similar seasonal behaviour with a distinct maximum of spring NO_2 VTCs. Further analysis indicates small GOME columns being systematically smaller than the ground-based ones. The influence of different shapes in the a priori and the ground-based NO_2 profile is analysed by considering AK information. It is moderate and indicates similar shapes of the profiles for clear sky conditions. Only for large GOME columns, differences between the profile shapes explain the larger part of the relative difference. In contrast, the other error sources give rise to the larger relative differences found towards smaller columns. Further, for the clear sky cases, errors from different sources are found to compensate each other partially. The comparison for cloudy cases indicates a poorer agreement between the columns (n=60, R=0.61). The mean relative difference between the columns is 60% with a standard deviation of 118% and GOME on average overestimating the ground-based columns. The clear improvement after inclusion of AK information (n=60, R=0.87) suggests larger errors in the a priori NO_2 profiles under cloudy conditions and demonstrates the importance of using accurate profile information for (partially) clouded scenes.

Correspondence to: D. Schaub
(daniel.schaub@empa.ch)

1 Introduction

Nitrogen dioxide (NO_2) is one of the most important air pollutants in the troposphere. It directly affects human health and plays a major role in the production of ground-level ozone (Seinfeld and Pandis, 1998; Finlayson-Pitts and Pitts, 2000). Furthermore, Solomon et al. (1999) pointed out the climatic effect of NO_2 as an absorber of solar radiation.

The bulk of the emitted NO_x ($\equiv$NO+NO_2) is of anthropogenic origin (Brasseur, 2003). The primarily emitted nitrogen oxide (NO) oxidises to NO_2 within seconds to minutes. The latter is removed from the troposphere after being

Published by Copernicus GmbH on behalf of the European Geosciences Union.

Table 1. Recent works on validation and/or intercomparison of space-borne NO_2 vertical tropospheric column densities with independent measurement data.

Author	Data: instrument (data provider)	Method (location)	Investigated period	Main result
Petritoli et al. (2004)	GOME (IUP Bremen)	Ground-based DOAS (Mt. Cimone, Italy)	2000–2001	GOME smaller by 14%
Petritoli et al. (2004)	GOME (IUP Bremen)	In situ measurements (Ferrara, Po-Valley)	2000–2001	Annual cycle reproduced by GOME
Heue et al. (2005)	SCIAMACHY (IUP Bremen)	AMAXDOAS (Alps, Po-Valley, Mediterranean)	Feb 2003	SCIAMACHY higher by 7%
Ordóñez et al. (2006)	GOME (IUP Bremen)	Surface (PBL) measurements combined with CTM-NO_2 profile shape (Lombardy)	1996–2002	GOME best agrees for slightly polluted stations
Heland et al. (2002)	GOME (IUP Bremen)	In situ aircraft NO_2 profile (Austria)	2 May 2001	GOME smaller by 3%
Martin et al. (2004)	GOME (CfA Cambridge, MA)	In situ aircraft NO_2 profiles (Texas, Tennessee)	June/July 1999 Aug/Sep 2000	GOME smaller by 8%

converted to nitric acid (HNO_3) which deposits (Kramm et al., 1995). During daytime, HNO_3 is formed through the reaction of NO_2 with the OH radical. During night time, a two step reaction chain forms nitrogen pentoxide (N_2O_5). The latter further reacts on surfaces and aerosol to HNO_3 (Dentener and Crutzen, 1993). The resulting NO_x lifetime is highly variable with an annual average boundary layer lifetime in the order of one day (Warneck, 2000). During photochemically active summer days, the lifetime can be reduced to only a few hours (e.g. Spicer, 1982). An increasing lifetime up to several days is found with increasing height in the troposphere (Jaeglé et al., 1998; Seinfeld and Pandis, 1998; Warneck, 2000). The mainly near-ground emissions of nitrogen species over industrialised areas, their production and loss reactions and meteorological transport lead to a distinct vertical tropospheric profile of NO_2 with enhanced mixing ratios in the polluted boundary layer.

In terms of air quality in Switzerland, the NO_x pollution situation has been improved during the last 15 years, but the annual limit values are still exceeded in polluted areas (BUWAL, 2004). Therefore, monitoring of nitrogen oxides still plays an important role in order to examine reduction measures. In addition to the monitoring networks around the globe, which provide ground-based in situ NO_2 measurements, space-borne spectrometers such as GOME (Burrows et al., 1999) provide area-wide information about the NO_2 vertical tropospheric column densities (VTCs) with a global coverage within only a few days.

1.1 Previous validation or comparisons studies with space-borne NO_2 VTCs

Typically, for validation purposes, space-borne trace gas columns are compared to ground-based or airborne column measurements. Some recent works on validation of NO_2 VTCs are summarised in Table 1. The comparison of GOME NO_2 VTCs with ground-based DOAS measurements carried out at Mount Cimone (Italy) yielded a good agreement for situations with horizontally homogeneous distribution of the pollution distribution (Petritoli et al., 2004). Heue et al. (2005) used the Airborne Multi Axis DOAS (AMAXDOAS) instrument on board the DLR Falcon to validate SCIAMACHY (Scanning Imaging Absorption Spectrometer for Atmospheric Chartography; Bovensmann et al., 1999) NO_2 VTCs over Italy in February 2003 and found SCIAMACHY values to be systematically higher than AMAXDOAS by approximately 7%.

Few comparisons including in situ data can be found in literature. The fundamental problem when comparing in situ measurements with column quantities arises from the fact that the latter integrate both horizontally and vertically, whereas in situ measurements provide point (ground-based site) or line (aircraft profile) information only. Petritoli et al. (2004) compared boundary layer in situ measurements from the Po-valley with GOME NO_2 VTCs and found a good qualitative correlation in the annual trend for high pollution episodes. Ordóñez et al. (2006) used 3-monthly averaged profile shapes from the chemistry transport model (CTM) MOZART-2 (Horowitz et al., 2003) that are scaled with ground-based in situ measurements for comparison with GOME NO_2 VTCs in the Lombardy region (Italy). Because the GOME NO_2 VTCs used in that study were retrieved based on a priori profiles from the same CTM, the focus has been on finding the best average boundary layer pollution level that scales the CTM column to best fit the GOME measurements. The best agreement has been found for average polluted situations.

In a case study, one in situ NO_2 profile measured from the DLR Falcon on a clear sky day above Austria has been used by Heland et al. (2002) for a comparison with GOME. They found a very small difference of -0.1×10^{15} molec cm^{-2} between the GOME and the in situ column. Martin et al. (2004) evaluated the consistency between GOME tropospheric NO_2 columns and averaged aircraft profile measurements not coinciding with the GOME observation. The latter two comparisons are the only published comparisons of tropospheric GOME NO_2 observations with independent tropospheric in situ profile measurements known to the authors. Furthermore, the comparison case study by Heland et al. (2002) is the only study that validates an individual GOME retrieval with a coincident aircraft profile.

Shortcomings of the validations/comparisons mentioned above arise from their necessary focus on very limited numbers of coincident pixels (or even single pixels) or their use of CTM derived NO_2 profile shapes. Furthermore, no study so far discussed the inclusion of averaging kernels for the comparison of space-borne NO_2 VTCs with independently derived NO_2 columns.

1.2 Present study

The present study compares GOME NO_2 VTCs from 1997 to June 2003 with a set of NO_2 columns derived from in situ NO_2 measurements in Switzerland. Ground-based in situ sites continuously measuring NO_2 at different altitudes in the Alpine region are used to obtain tropospheric NO_2 profile information. New aspects of the present work are

- the first long-term comparison of GOME NO_2 VTC data retrieved by KNMI/BIRA (available at the Tropospheric Emission Monitoring Internet Service (TEMIS) web site http://www.temis.nl) with independently derived tropospheric NO_2 profiles,
- the NO_2 profile/column construction from ground-based in situ measurements,
- the comparison through inclusion of averaging kernel information,
- the first investigation of tropospheric NO_2 retrieval errors under cloudy situations.

Both the space-borne and the ground-based in situ measurement data are described in Sect. 2. The detailed method of deducing the tropospheric NO_2 column from ground-based in situ measurements is introduced in Sect. 3. Sections 4 and 5 discuss the ground-based in situ columns (hereafter called ground-based columns) and the comparison between the latter and GOME NO_2 VTCs for anticyclonic clear sky and for cloudy conditions, respectively.

2 Measurement data

2.1 KNMI/BIRA GOME tropospheric NO_2 observations

The Global Ozone Monitoring Experiment (GOME) instrument on board ESA's ERS-2 satellite is a nadir-viewing spectrometer that measures upwelling radiance from the atmosphere and solar irradiance. The satellite instrument takes observation at approximately 10:30 h local time and individual pixels cover an area of 320×40 km^2. The GOME principles are described by Burrows et al. (1999).

The GOME NO_2 VTCs studied in this work are the result of a collaboration of KNMI and BIRA/IASB. GOME NO_2 data are publicly available on a day-by-day basis from 1 April 1996 until 30 June 2003 via ESA's TEMIS project (http://www.temis.nl).

The first step of the retrieval is taken by BIRA/IASB based on the Differential Optical Absorption Spectroscopy (DOAS) technique (Vandaele et al., 2005). It consists of the fitting of a modelled spectrum to a GOME-measured reflectance spectrum in the spectral window from 426.3–451.3 nm. This modelled spectrum takes into account the spectral features of absorption by NO_2, O_3, O_2-O_2 and H_2O, and describes scattering on clouds, aerosols and air molecules by a low-order polynomial. The result of this first step is the so-called slant column density (SCD) of NO_2. This SCD should be interpreted as the column integral of absorbing NO_2 molecules along the effective photon path from the sun through the atmosphere to the GOME spectrometer.

The second step of the retrieval is the separation of the stratospheric contribution from the total SCD (Boersma et al., 2004). This is achieved with a data-assimilation approach. In the data-assimilation step, NO_2 in TM4 (Dentener et al., 2003) is made consistent with observed SCDs over unpolluted areas. Subsequently, the stratospheric estimate is subtracted from the total SCD. Note that the residual tropospheric slant column (SCD_{trop}) is insensitive to calibration errors, as any offsets in the total and stratospheric SCDs will cancel in the subtraction. Finally, the SCD_{trop} is converted into a VTC by applying the tropospheric air mass factor. The latter is calculated with the Doubling Adding KNMI (DAK) radiative transfer model (Stammes, 2001) and represents the best estimate of the length of the effective photon path for a particular retrieval scene. The tropospheric air mass factor depends on a priori assumptions on the state of the atmosphere, including surface albedo, cloud fraction, cloud height and the vertical distribution of NO_2. For KNMI retrievals, a priori NO_2 profiles for every location and all times are obtained from the TM4 CTM. Cloud parameters are taken from the Fast Retrieval Scheme for Clouds from the Oxygen A band (FRESCO) algorithm (Koelemeijer et al., 2001).

During the above mentioned steps, a number of error sources can lead to inaccurate retrieval results. The error budget of the tropospheric vertical columns has been studied extensively in Boersma et al. (2004). Over polluted regions

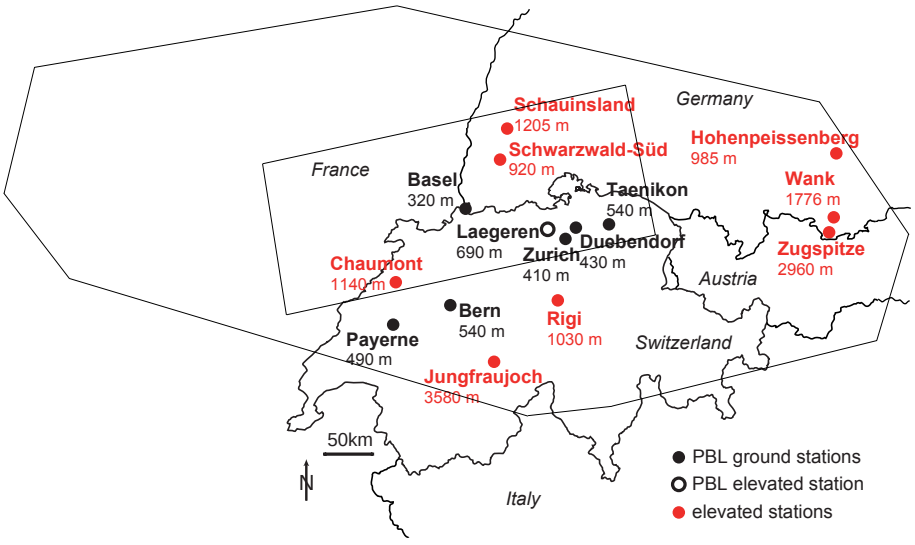

Fig. 1. Ground-based in situ measurement stations in the PBL and at elevated sites used in the present study. GOME pixels with its centre coordinates located within the rectangular frame above northern Switzerland are used for the comparison. The resulting region covered by the GOME pixels of interest is additionally denoted.

as considered in the present study, errors in the SCD (e.g. due to instrument noise, laboratory reference spectra errors, interference with other absorbers and Ring effect) and in the separation of the stratospheric contribution from the total SCD play a minor role. For such regions, the most critical error source is the calculation of the tropospheric air mass factor. The latter depends on the a priori assumed NO_2 profile shape, the cloud fraction, the cloud top height, the surface spectral reflectance (surface albedo, e.g. near land-snow boundaries) and the aerosol optical thickness profile. Based on theoretical error sources and for cloud free conditions, Boersma et al. (2004) estimated mean tropospheric air mass factor uncertainties for polluted regions ($>1.0\times10^{15}$ molec cm^{-2}) of 15%, 2%, 15% and 9% due to the model parameters cloud fraction, cloud top height, surface albedo and a priori NO_2 profile shape, respectively. The total mean uncertainty for the tropospheric air mass factor is estimated to be 29%, resulting in a total mean uncertainty for the NO_2 VTCs of 35–60%. No error due to aerosol is included for the KNMI NO_2 retrievals. Boersma et al. (2004) have argued that the presence of aerosol modifies the retrieval of cloud fraction and height with the FRESCO algorithm. A comparison of the expected aerosol correction factor versus the actual correction effect from the cloud retrieval has shown that even for a large aerosol optical thickness, the expected correction factor and actual correction effect agree to within 10%. Boersma et al. (2004) therefore suggest that cloud algorithms implicitly correct for aerosol through their modified cloud fraction and height.

Due to the cloud parameters that can be affected by uncertainties and the simplifying assumption that the cloud can be approximated as a Lambertian reflector with an effective cloud top height, larger errors are expected for the retrieval of cloudy scenes. The DAK radiative transfer model (Stammes, 2001) accounts for multiple scattering, but a detailed quantitative error analysis has so far not been carried out for these issues. Preliminary simluations with the DAK showed that light penetrates quite far into the cloud and the NO_2 signal can originate from the upper half of the cloud. The FRESCO effective cloud top height represents this by putting the effective reflective surface below the real cloud top. However, the above mentioned small error due to uncertainties in the cloud top height for clear sky conditions can be thought to increase when the clouds are associated with, e.g., frontal activity. The vertical mixing of near ground pollution can then lead to a higher NO_2 abundance near the cloud top, which induces a larger error compared to the clear sky situation with the bulk of the NO_2 residing well below the cloud height. An explicit quantification of the error of cloudy NO_2 VTCs has so far not been given in literature, but we estimate it to be in the order of 100%.

2.2 Ground-based in situ measurements

The Swiss National Air Pollution Monitoring Network (NABEL) provides long-term ground-based in situ measurements. Planetary boundary layer (PBL) stations representative for different pollution levels as well as stations located at different altitudes are included in this study (Fig. 1). In order to get more information about higher levels in the lower troposphere, two Alpine stations operated by the Umweltbundesamt (Germany) are further taken into account (Fig. 1). Details about measurement devices and locations can be found in Umweltbundesamt (2003), BUWAL (2004) and Empa (2005).

NO_2 is measured with the chemiluminescence technique (Navas et al., 1997; Clemitshaw, 2004) that includes the conversion of NO_2 to NO. While the Jungfraujoch and the Hohenpeissenberg stations are equipped with photolysis converters that allow a selective measurement of NO_2, the other stations are measuring with the molybdenum conversion technique. It is known that these catalytic surface converters are sensitive not only to NO_2, but also to other nitrogen species such as PAN, HNO_2, HNO_3 and particulate nitrate (Zellweger et al., 2003; Clemitshaw, 2004). In order to account for this non-selective NO_2 measurements at most of the stations used in this study, campaign results of simultaneous measurements based on both the photolysis and the molybdenum conversion technique at a PBL station (Taenikon) and an elevated station (Rigi) are used to determine correction factors (Sect. 3.1.3). A similar approach has been used in Ordóñez et al. (2006).

3 Methods

3.1 Column calculation from ground-based in situ measurements

The mountainous terrain in the Alpine region allows operating ground-based in situ measurement sites at different altitudes. These stations are assumed to detect NO_2 concentrations that are approximately representative for the appropriate height in the (free) troposphere over flat terrain. These measurements, together with boundary layer in situ measurements and an assumed mixing ratio at 8 km, are used to construct NO_2 profiles. The latter can subsequently be integrated to tropospheric NO_2 columns. Deducing tropospheric profile and column information from ground-based in situ measurements is not straightforward because the issue of representativeness has to be taken into account carefully. The following subsection alludes to the principle method of constructing the NO_2 profile from the in situ measurements. Afterwards, issues of representativeness and errors are discussed.

3.1.1 Deducing the NO_2 profile/column

The stations shown in Fig. 1 are used to deduce the tropospheric NO_2 profile. Every station provides a 3-h NO_2 average concentration calculated from 09:00 to 12:00 UTC (i.e. around the GOME overpass at 10:30 h local time). Concentrations not measured with a photolysis converter are corrected with correction factors accounting for the interference in the NO_2 measurement (Sect. 3.1.3). Because we are going to use averaging kernel (AK) information with a higher vertical resolution than covered by the various stations, the ground-based profile is divided into partial subcolumns to match the vertical resolution of the AK.

The NO_2 in the upper troposphere is neglected because, due to the generally smaller mixing ratios and decreasing pressure with height, the effective NO_2 molecule number concentration at these levels is small compared to the NO_2 in the lower troposphere (Sect. 3.1.2). The elevated stations (above 900 m a.s.l.) together with a near-zero NO_2 mixing ratio of 0.02 ppb at 8 km are first used for a curve fit, which can be regarded as an average profile given by the elevated stations. The curve fit is based on a power law equation resulting in a hyperbolic profile shape. Subsequently, the in situ measurements are assigned to the appropriate height intervals in the following way:

Above 900 m a.s.l. (i.e. for the elevated part of the profile), the partial subcolumns are given as either the mean NO_2 concentration from the stations within the height interval, or the NO_2 concentration from the curve fit if no elevated station is available. Subcolumns for height intervals below 900 m a.s.l. are obtained from linear interpolation between the 900 m NO_2 concentration (resulting from the curve fit) and the remote and elevated PBL station Laegeren, as well as between the latter and the average PBL NO_2 concentration at the mean Swiss Plateau ground height of 400 m a.s.l.

To determine the average PBL NO_2 concentration within an individual GOME pixel, spatial inhomogeneities of the NO_x emissions must be taken into account. To do this, we assume that the NO_x emissions are proportional to the population density distribution. This assumption has previously been proven to be useful (Schaub et al., 2005). For the GOME pixel under consideration, the $0.25° \times 0.25°$ population density grid elements enclosed in the pixel are sorted into four different (arbitrarily chosen) pollution classes c (Table 2). Each class is described by a population density range and appropriate measurement stations representative for the pollution level (Empa, 2005). From the numbers p_c of population density grid elements in each class, the average PBL NO_2 concentration within the GOME pixel is calculated as a weighted mean concentration using the appropriate stations representative for the pollution class:

$$[NO_2]_{pbl} = \frac{\sum_{c=1}^{4} [NO_2]_c \cdot p_c}{\sum_{c=1}^{4} p_c}.$$

Table 2. NO_2 pollution classes represented by population density ranges and associated representative Swiss Plateau (boundary layer) ground measurement stations.

Pollution class (c)	Population density [km^{-2}]	Representative measurement station
Very remote	<30	None (0.5× remote)
Remote	30–499	Taenikon, Payerne
Polluted	500–999	Duebendorf, Basel
Highly polluted	>1000	Berne, Zurich

Measurement gaps at the ground measurement sites occasionally prevent the use of all 15 stations from Fig. 1 for the NO_2 profile construction. On average, 13 stations are available for deducing a profile.

The ground-based columns described so far are derived for an NO_2 profile starting at ground-height (Swiss Plateau). The Alpine terrain is excluded as far as possible (Fig. 1). Nevertheless, the GOME pixels always cover a non-flat terrain in the present study area and the signal can be seen as a superposition of signals associated with columns of different vertical extension. To reproduce this in the ground-based columns, the topography of the Alpine Local Model (aLMo, operational numerical weather forecast model of MeteoSwiss) with a resolution of $7\,km \times 7\,km$ is used to calculate a mean (or effective) surface height within the GOME pixel. The part of the ground-based NO_2 VTC located above this height is finally used as the representative ground-based column for the further comparison.

3.1.2 Representativity of the constructed profiles

The representativity of the profiles constructed by the method described in Sect. 3.1.1 for the true atmospheric NO_2 profile over Northern Switzerland may be limited as a consequence of the following:

A) The vertical distribution of NO_2 within the PBL may not be well captured.

B) Inhomogeneities of NO_2 over the size of a GOME pixel may not be well captured.

C) Elevated stations may not be representative for the NO_2 at corresponding heights.

Here we shortly discuss each of these issues and their possible impact on the representativity of our constructed profile.

A) Vertical NO_2 distributions within the PBL are variable. For instance, Pisano et al. (1997) have shown NO_2 to be homogeneously distributed within the well-mixed convective boundary layer (CBL) in summer. On the other hand, Herwehe et al. (2000) modelled the boundary layer NO_2 vertical distribution and found that also within a summertime well-mixed boundary layer, the NO_2 can exhibit a strong decrease with height because the NO_2 lifetime can be shorter than the typical mixing time scale in the CBL (Spicer, 1982; Herwehe et al., 2000). Therefore, in situ measurements from an additional PBL station that is located on a mountain ridge about 250 m above the ground height of the Swiss Plateau (Laegeren, Fig. 1) are used (Sect. 3.1.1).

B) Due to the distances between the elevated stations (Fig. 1) and the relatively short chemical lifetime of NO_2 it is obvious that small-scale structures of the 3-dimensional NO_2 distribution in the free troposphere are difficult to catch by our comparison approach. Furthermore, neglecting the upper troposphere NO_2 above 8 km might not apply for columns affected by lightning or deep convection where NO_2 column enhancements of up to 1.0×10^{15} molec cm^{-2} were reported (Boersma et al., 2005; Choi et al., 2005). However, such events occur only occasionally and are not expected during anticyclonic clear sky days. During such conditions, Ridley et al. (1998) conducted simultaneous flights measuring NO_x profiles up to 5000 metres asl representative locally (flight patterns with sides of 15–20 km) and regionally (horizontal flight distances of around 200 km) and qualitatively described a good agreement between the two profiles. Although these measurements were carried out at lower latitudes (30° to 34° N), we suggest that the focus on anticyclonic conditions supports our assumption of the NO_2 being homogeneously distributed on clear sky high pressure days also in mid latitudes.

It can be expected that larger inhomogeneities occur under cloudy conditions when frontal transport takes place. However, such conditions can also lead to spatially extended air masses, which are relatively well-mixed (Schaub et al., 2005). We furthermore note the large GOME footprint, which averages over a large area. Finally, the averaging time window for the ground-based measurements from 09:00–12:00 UTC to a certain extent averages out horizontal inhomogeneities.

C) Measurements from elevated stations may not be representative for the NO_2 at corresponding heights over flat terrain. It is known that, mainly during summertime convective conditions in the Alpine region, even high-alpine stations often detect pollution that reaches the site due to thermally induced upslope transport in the afternoon (Forrer et al., 2000; Lugauer et al., 2000; Nyeki et al., 2000; Zellweger et al., 2003). However, because of the GOME overpass around 10:30 h local time in the morning with an averaging time window for the ground-based in situ NO_2 measurements from 09:00–12:00 UTC, this is not expected to be a major issue for the present comparison. During the winter season, high-alpine sites have shown to be decoupled from the boundary layer during anticyclonic conditions, and thus representing the undisturbed free troposphere (Lugauer et al., 2000). Hence, we expect the high-alpine measurements taken during the GOME overpass time to be representative for free tropospheric NO_2 levels.

Stations located around 1000 m a.s.l., on the other hand, are affected by polluted air masses already before noon. Nevertheless, we suggest these stations to be representative. Three cases can be distinguished:

1) On clear sky summer days, the boundary layer height grows very fast and can reach heights of 1000 m above ground already before noon (Nyeki et al., 2000; Seibert et al., 2000). Because in Switzerland a station located at 1000 m a.s.l. lies around 500 m above the ground (Swiss Plateau) effectively, the site can be thought to represent the PBL NO_2 levels.

2) During wintertime, the PBL often does not reach a height of 500 m above ground (e.g. Seibert et al., 2000).

In fact, the stations around 1000 m a.s.l. used in this study often measure low concentrations during clear sky winter days. Therefore, in winter, measurements at 1000 m a.s.l. are thought to be representative for free tropospheric NO_2 levels.

3) In spring, the upslope pollution transport could lead to pollution located above the PBL height over flat terrain, and one might argue that a station is no longer representative for the corresponding height level over the flat terrain. On the other hand, GOME measurements over the northern part of Switzerland should detect such events to a certain extent. The region is surrounded by mountainous areas with the Alps and the foothills of the Alps in the south/east and the Jura/Black Forest mountains in the north. Lugauer et al. (1998) argued that pollution once lifted can reside in the free troposphere. A measurement site affected by thermal upslope pollution transport can therefore be regarded to be representative for the "disturbed" free troposphere on a regional scale at least. Thus, with the five measurement sites around 1000 m a.s.l. and situated at five different locations within the region of interest and with different slope expositions and surroundings included in this study, the overall pollution situation should – on average – be captured. Nevertheless, NO_2 concentration differences between these five measurements are taken as a measure for inhomogeneities and thermally induced upslope transport (Sect. 3.1.4).

3.1.3 Interference in ground-based in situ NO_2 measurements

Ground measurement stations equipped with molybdenum converters overestimate the NO_2 concentration due to non-selective conversion of nitrogen species (Clemitshaw, 2004). Due to the complex chemistry of nitrogen species, the difference between the selective and the non-selective NO_2 measurement strongly depends on meteorological conditions and the distance of the station from major emission sources. Campaign results of two stations that simultaneously measured with both the photolysis (selective NO_2 measurement) and the molybdenum conversion technique (non-selective NO_2 measurement) are used to compute a correction factor: a boundary layer station (Taenikon, 540 m a.s.l.) and an elevated site (Rigi, 1030 m a.s.l.) for the correction of measurements from boundary layer and elevated stations, respectively. The correction factor is calculated as

$$cf = \frac{[NO_2]_{\text{photolysis}}}{[NO_2]_{\text{molybdenum}}}.$$

The elevated stations at Jungfraujoch and Hohenpeissenberg are equipped with selective (photolysis) converters and are, therefore, not corrected. Due to the seasonal variation in the photochemical activity monthly averaged correction factors are calculated for NO_2 measurements from 09:00 to 12:00 UTC (Fig. 2).

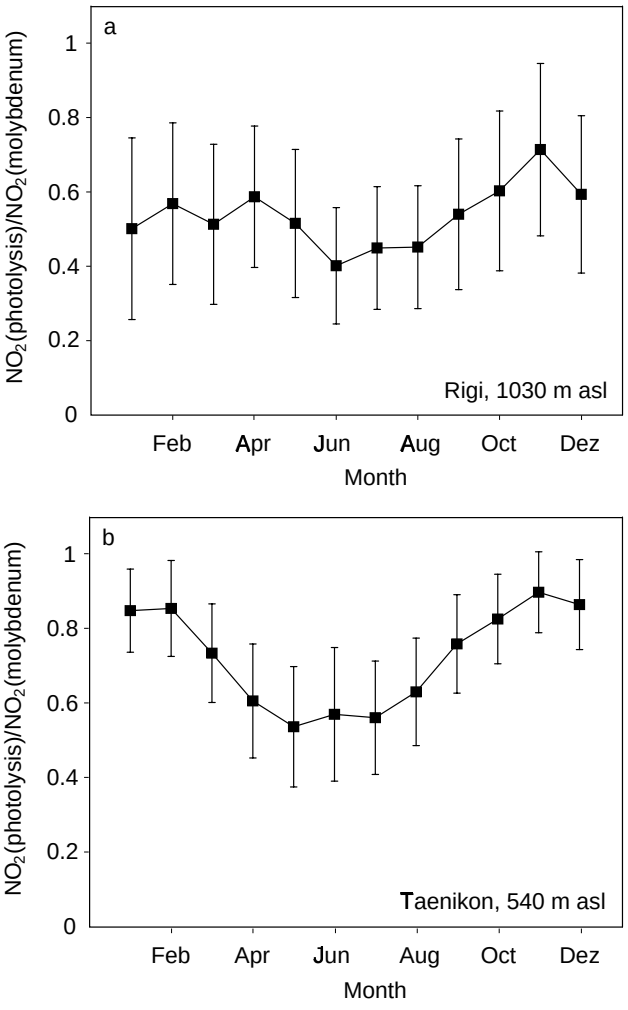

Fig. 2. Monthly mean ratios (and standard deviations) between NO_2 concentrations measured from 09:00 to 12:00 UTC on clear sky days with photolysis and with molybdenum conversion technique for the elevated station Rigi **(a)** and the PBL station Taenikon **(b)**.

3.1.4 Error estimation for ground-based NO_2 VTCs

This section discusses the main error sources in the ground-based columns and suggests a simple "worst case" error estimate.

1) The error due to the selected pollution classes for determining the average PBL NO_2 concentration (Sect. 3.1.1) is very small. This is because the weak impact due to changing pollution classes is further decreased by the use of an effective surface height at the GOME pixel location. The effective surface height does not reach down to the Swiss Plateau height. Based on different choices for the pollution classes, relative uncertainties in the resulting ground-based NO_2 VTCs of only a few percent are found. This error is very small compared to the other errors and is therefore neglected.

2) Errors in the vertical NO_2 distribution in the PBL, the representativity of elevated stations for the free troposphere,

and the assumption of horizontal homogeneity of NO_2 in the free troposphere as discussed in Sect. 3.1.2 can be thought to be a major error source for the estimated ground-based columns. A crude overall estimation of this error is based on the five measurement sites located at altitudes of between 920 m a.s.l. and 1205 m a.s.l. (Fig. 1). On the one hand, these sites strongly affect the NO_2 profile deduced from the ground stations. On the other hand, the stations are located in an altitude range of only 285 m. Therefore, the standard deviation of their NO_2 concentrations is taken as an indicator for horizontal inhomogeneities and the non-representativeness of certain stations due to, e.g., thermal upslope transport of pollution. The resulting uncertainty of the ground-based column is determined with a sensitivity test, where the five concentrations are enhanced simultaneously by the calculated standard deviation. This can be seen as a "worst case" scenario. The average resulting uncertainty is in the order of 20%, with an upper limit of approximately 50%.

3) Another significant error arises from the non-selective NO_2 measurement techniques used at most of the ground stations. Correction factors calculated for a selected station might not be representative for another station. Furthermore, meteorological conditions affect the correction factor, as indicated by the large standard deviations in the monthly correction factors (Fig. 2). For the error estimation, the change in the ground-based columns is calculated with monthly correction factors that are simultaneously changed by their standard deviations ("worst case" scenario). The average resulting error is in the order of 30%, with an upper limit of approximately 35%.

Finally, because dependence between these errors cannot be excluded, the error is assumed to be additive and is calculated as the sum of the two main error contributions, amounting to a conservative estimate of the average error of around 50%. This error will consist of both systematic error contributions – which will amount to a bias – and random contributions. The same holds for the GOME retrievals.

3.2 Space-borne to ground-based comparison methods

Following Palmer et al. (2001) and Boersma et al. (2004), the retrieved GOME NO_2 VTC (VTC_{GOME}) is calculated as

$$VTC_{\mathrm{GOME}} = \frac{SCD_{\mathrm{trop}}}{AMF_{\mathrm{trop}}(\boldsymbol{x}_a, \boldsymbol{b})} = \frac{SCD_{\mathrm{trop}} \cdot \sum_l x_{a,l}}{\sum_l m_l(\boldsymbol{b}) \cdot x_{a,l}}. \quad (1)$$

SCD_{trop} denotes the tropospheric slant column density, which is the difference between the total SCD resulting from fitting the reflectance spectrum measured from the satellite and a stratospheric SCD. For KNMI retrievals, the latter is determined by data assimilation of observed SCDs in a chemistry-transport model (Eskes, 2003). AMF_{trop} is the tropospheric air mass factor, which is defined as the ratio between SCD and VTC. $x_{a,l}$ are the layer specific subcolumns from the a priori profile $\boldsymbol{x}_a$, and m_l are the altitude-dependent scattering weights. The latter are calculated with a radiative transfer model and best estimates for forward model parameters $\boldsymbol{b}$, describing surface albedo, cloud parameters (fraction, cloud top pressure) and GOME pixel surface pressure.

If independently measured tropospheric NO_2 profile information $\boldsymbol{x}_{\mathrm{ind}}$ is available, there are different possibilities for comparison, each having its own meaning.

3.2.1 First comparison approach

The straightforward first comparison approach (hereafter called first comparison) uses the independently measured NO_2 profiles that are directly integrated to tropospheric columns (VTC_{ind}):

$$VTC_{\mathrm{ind}} = \sum_l \boldsymbol{x}_{\mathrm{ind},l}, \quad (2)$$

with $\boldsymbol{x}_{\mathrm{ind}}$ the ground-based NO_2 profile and l the tropospheric layers. The relative difference between the two columns with respect to the ground-based column is calculated as

$$\Delta_0 = \frac{VTC_{\mathrm{GOME}} - VTC_{\mathrm{ind}}}{VTC_{\mathrm{ind}}} = f(SCD_{\mathrm{trop}}, m_l(\boldsymbol{b}), \boldsymbol{x}_a, \boldsymbol{x}_{\mathrm{ind}}). \quad (3)$$

Δ_0 is a measure that will be comparable to other validation studies where, typically, relative differences are calculated with respect to the "true" columns. Δ_0 depends on all parameters affecting the retrieval and the ground-based column calculation, including differences in the shapes of the a priori profile $\boldsymbol{x}_a$ and the ground-based profile $\boldsymbol{x}_{\mathrm{ind}}$.

A second relative difference is calculated with respect to the GOME column (and the latter therefore being the denominator in Eq. 4):

$$\Delta_1 = \frac{VTC_{\mathrm{GOME}} - VTC_{\mathrm{ind}}}{VTC_{\mathrm{GOME}}} = f(SCD_{\mathrm{trop}}, m_l(\boldsymbol{b}), \boldsymbol{x}_a, \boldsymbol{x}_{\mathrm{ind}}). \quad (4)$$

The reason for defining Δ_1 will become obvious in the next section (where Δ_1 is further divided into two contributions).

3.2.2 Second comparison approach

Eskes and Boersma (2003) applied the general formalism developed by Rodgers (2000) for the case of DOAS retrievals that are typically done for weak absorbers ($\tau < 1$) and generally give column integrals of the concentration species only. The averaging kernel (AK) vector describes the relation between the true vertical distribution of a species and the retrieved vertical column. Multiplying the ground-based NO_2 profile with the AK yields $VTC_{\mathrm{ind\_AK}}$:

$$VTC_{\mathrm{ind\_AK}} = \sum_l a_l(\boldsymbol{x}_a, \boldsymbol{b}) \cdot x_{\mathrm{ind},l}, \quad (5)$$

with a_l the AK element for layer l. Following Boersma et al. (2004) the relative difference between $VTC_{\mathrm{ind\_AK}}$ and the GOME column is

$$\Delta_2 = \frac{VTC_{\mathrm{GOME}} - VTC_{\mathrm{ind\_AK}}}{VTC_{\mathrm{GOME}}} = f(SCD_{\mathrm{trop}}, m_l(\boldsymbol{b}), \boldsymbol{x}_{\mathrm{ind}}). \quad (6)$$

Unlike Δ_1, Δ_2 is no longer influenced by the a priori NO_2 profile $\boldsymbol{x}_a$ (Eskes and Boersma, 2003). For the interpretation of the second comparison approach (hereafter called second comparison), it is helpful to reformulate Eq. (6). Following Eskes and Boersma (2003), the expression for a_l can be written as

$$a_l = \frac{m_l(\boldsymbol{b})}{AMF_{\text{trop}}(\boldsymbol{x}_a, \boldsymbol{b})}. \quad (7)$$

Including Eqs. (1), (5) and (7) in Eq. (6) and reformulating yields

$$\begin{aligned}\Delta_2 &= \frac{SCD_{\text{trop}} - \sum_l m_l(\boldsymbol{b}) \cdot x_{\text{ind},l}}{SCD_{\text{trop}}} \\ &= f(SCD_{\text{trop}}, m_l(\boldsymbol{b}), \boldsymbol{x}_{\text{ind}}).\end{aligned} \quad (8)$$

Equation (8) demonstrates that the second comparison amounts to a comparison of slant column densities. Because the AMF_{trop} divides out, the a priori NO_2 profile $\boldsymbol{x}_a$ no longer contributes to Δ_2. Further, the second term of the numerator in Eq. (8) indicates the slant column to be a linear sum of signal contributions from all individual layers, which is a valid approximation for weak absorbers (Eskes and Boersma, 2003; Boersma et al., 2004). Therefore, the above equation can be interpreted as how well the ground-based NO_2 profile together with the scattering weights m_l can describe SCD_{trop}.

In the previous section, we introduced Δ_1, which depends on all parameters affecting the comparison. Because the same denominator appears in both Δ_1 and Δ_2, we can write

$$\Delta_1 = \Delta_2 + \Delta_3. \quad (9)$$

Therefore, Δ_1 can be split into two contributions: Δ_3 that depends on differences between the shapes of the a priori and the ground-based NO_2 profile, and Δ_2 that is due to uncertainties in both the remaining retrieval parameters and the ground-based NO_2 profile. In the following, Δ_1 and Δ_2 are calculated from the first and the second comparison, respectively. Δ_3 is calculated as the difference between Δ_1 and Δ_2.

4 Results for clear sky (anticyclonic) conditions

4.1 NO_2 VTCs from ground-based in situ measurements

From 1997 to June 2003, ground-based NO_2 VTCs are calculated for 335 days with both clear sky conditions (MeteoSwiss, 1985) and GOME NO_2 VTC data above northern Switzerland (Fig. 1) available. Figure 3 shows two example NO_2 profiles deduced from ground-based in situ measurements for 3 December 1999 and for 22 July 2002. The December example shows a typical anticyclonic winter case where an inversion prevents vertical mixing and the NO_2 is concentrated in the narrow PBL. The more effective mixing in the July example and the reduced chemical lifetime of NO_2 during the warm season leads to a boundary layer concentration being a factor of 10 lower than for the winter case.

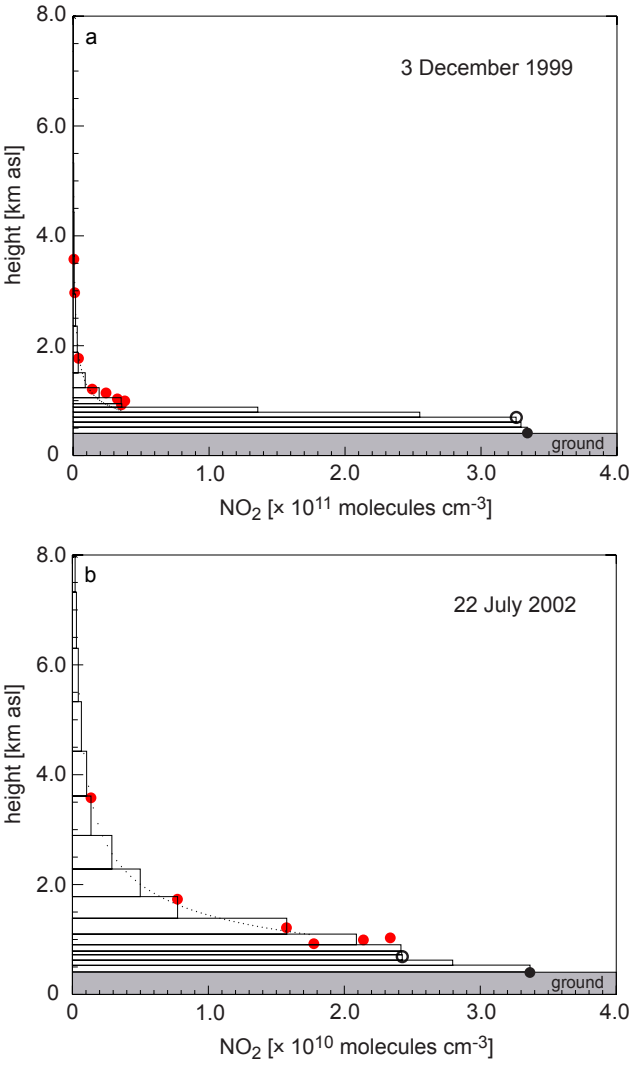

Fig. 3. Example NO_2 profiles for 3 December 1999 **(a)** and for 22 July 2002 **(b)**. Note the different x-axis. The two PBL values (filled and open black circles) are derived from the PBL ground and elevated stations in Fig. 1. The red data points are derived from the elevated stations located in Southern Germany and Switzerland (Fig. 1). Occasionally, measurement gaps prevent the use of all available measurement sites for the profile determination.

Employing 12:00 UTC radio soundings from Payerne (Switzerland; e.g. Beyrich et al., 1998), PBL heights are calculated with the parcel method (Troen and Mahrt, 1986; Holtslag et al., 1990) and the Richardson number method (Vogelezang and Holtslag, 1996). With these PBL heights, the annual mean fractions of NO_2 located within and above the PBL are calculated to be 69% and 31%, respectively, for the ground-based NO_2 profiles reaching down to the Swiss Plateau height. For comparison, Martin et al. (2004) reported a summertime fraction of nearly 75% of the tropospheric

Table 3. Fraction of NO_2 vertical column density (VTC) above and within the planetary boundary layer (PBL) calculated from the ground-based NO_2 VTC alone and multiplied with averaging kernel (AK) information. The whole ground-based NO_2 columns are considered (i.e. reaching down to the height of the Swiss Plateau).

	Ground-based NO_2 VTC	Ground-based NO_2 VTC×AK
Fraction of NO_2 above PBL	31±14%	55±16%
Fraction of PBL NO_2	69±14%	45±16%

NO_2 below 1500 m in Houston and Nashville, USA. Ordóñez et al. (2006) found an average NO_2 fraction below 1000 m in the northern Italy region of more than 80%. The reason for the lower PBL column fraction in the area of northern Switzerland and surroundings is the lower NO_2 pollution compared to northern Italy.

The GOME nadir UV-VIS sensor exhibits a higher sensitivity towards NO_2 located in higher atmospheric layers. To check the "satellite's view", the layer-specific NO_2 ($x_{\mathrm{ind},l}$) is multiplied with the altitude-dependent scattering weight m_l to get the within/above PBL NO_2 SCDs as seen from satellite. Employing averaging kernel information and the AMF_{trop} and following Eq. (7) in Sect. 3.2.2 the NO_2 SCD above the PBL is

$$SCD_{\mathrm{NO_2 above\,PBL}} = \sum_{\text{above PBL}} x_{\mathrm{ind},l} \cdot m_l(\boldsymbol{b}) = AMF_{\mathrm{trop}} \cdot \sum_{\text{above PBL}} x_{\mathrm{ind},l} \cdot a_l. \quad (10)$$

Similarly the total tropospheric NO_2 SCD, the PBL NO_2 SCD and, subsequently, the fractions within and above the PBL are calculated. Table 3 indicates that, on average, 55% of the signal measured by the space-borne instrument in the present study area originates from above the PBL, although only 31% of the NO_2 resides there in reality. The PBL contribution is 45%. Because the following comparison employs the part of the ground-based profile located above the mean topography height within a GOME pixel, the importance of the PBL contribution is further reduced. This emphasises the importance of the elevated stations for the present comparison.

4.2 Comparison for clear sky conditions

For the clear sky comparison between the GOME and the ground-based NO_2 VTCs, we have used the following criteria:

- GOME pixel location above northern Switzerland (Fig. 1),
- Alpine weather statistics parameters (MeteoSwiss, 1985) indicate anticyclonic conditions and the absence of clouds,
- GOME pixel cloud fraction from FRESCO algorithm (Koelemeijer et al., 2001) $\leq$0.1,
- SCD_{trop}/SCD>10%.

The last condition is enforced because for some cases unrealistically small GOME NO_2 VTCs are retrieved when the total SCD and the (assimilated) stratospheric SCD are very similar. For such cases, uncertainties in the stratospheric SCD generate a strong change in the tropospheric VTC, although the error of the stratospheric SCD is small and estimated to not exceed 0.2×10^{15} molec cm^{-2} (Boersma et al., 2004). This criterion rejects 20 GOME pixels from the comparison.

Based on GOME NO_2 VTCs from 1997 to June 2003 and following the above conditions a data set of 157 clear sky columns is extracted for the subsequent comparison.

4.2.1 First comparison

Figure 4a shows the scatter plot for the first comparison between VTC_{GOME} and VTC_{ind}. A weighted orthogonal regression is used instead of a simple linear regression, because both data sets are affected by errors (York, 1966). GOME NO_2 VTCs 1-sigma errors are taken from the TEMIS data file where, for each individual pixel, an error estimate is given (Boersma et al., 2004). The error assessment for each of the ground-based VTCs follows Sect. 3.1.4. Interestingly, the independently calculated error estimates for the two data sets are very similar: the mean GOME 1-sigma error and the mean ground-based VTC error are determined to be 56% and 49%, respectively. The slope and the intercept (with their standard deviations) are calculated to be 1.15 (±0.22) and −1.23 (±0.90), respectively, with a correlation coefficient R=0.70. Although there is a good general agreement between the two column data sets, the regression indicates a tendency of small GOME columns slightly underestimating the corresponding ground-based columns. This is further discussed in Sect. 4.3.2.

The seasonal behaviour is very similar (Fig. 4b). The small summertime NO_2 VTCs mirror the shorter chemical lifetime of NO_2 during photochemically active summer days (Spicer, 1982; Warneck, 2000). Furthermore, both column data sets independently detect the largest NO_2 VTCs during the spring season. Moxim et al. (1996) simulated the global tropospheric chemistry of peroxyacetyl nitrate (PAN) and NO_x and found regional NO_x spring maxima in the lower troposphere of the northern hemisphere. This is consistent with Penkett and Brice (1986) who suggested the measured PAN maximum in spring to be due to the accumulation of precursor substances (such as NO_x) during the cold season and subsequent photochemistry in spring leading to enhanced photooxidants such as PAN and ozone. Note, however, that the latter studies focused on a larger region than middle Europe. Nevertheless, due to their vertical extension, the GOME columns investigated here could be affected by

air masses representative for a larger spatial scale similarly to elevated measurement sites in the Alpine region. At such sites, the NO_2 concentration also shows a spring maximum (Staehelin et al., 2000; BUWAL, 2004). The good agreement for the spring NO_2 VTCs can be seen as a crude validation of both NO_2 column data sets.

The qualitative comparison between the GOME NO_2 VTCs and the PBL NO_2 concentrations (derived following Sect. 3.1.1, Fig. 4c) shows that a proper comparison requires information on the vertical NO_2 distribution. As expected, the near-ground NO_2 concentrations are highest in winter, mainly due to near-ground inversions that often occur during this season. In summer, the near-ground NO_2 concentrations are lowest because of stronger photochemical activity and vertical mixing leading to dilution. The NO_2 VTC spring maximum is not mirrored in the average PBL NO_2 concentration.

4.2.2 Second comparison

The second comparison is shown in Fig. 5. Again, a weighted orthogonal regression is calculated based on both the GOME NO_2 VTC 1-sigma errors and the ground-based NO_2 VTC errors estimated following Sect. 3.1.4. The mean errors for both data sets are again similar, with a mean GOME 1-sigma error of 48% and a mean error for the ground-based VTCs of 45%. The resulting slope and intercept (with their standard deviations) are calculated to be 1.01 ($\pm$0.16) and $-$0.83 ($\pm$0.70), respectively, with a correlation coefficient R=0.74. The inclusion of AK information tends to improve the comparison. Nevertheless, the offset still gives evidence for small GOME columns slightly underestimating the corresponding ground-based columns.

It should, however, be noted that the orthogonal regression depends on the errors attributed to the data sets. These errors are estimates that also have their uncertainties. Tests performed with varying errors indicated somewhat changing results for slopes and offsets. However, independent from changes in the errors, the slopes of the orthogonal regression together with their standard deviations indicate, that the multiplication with the AK has a relatively weak impact. This is due to – on average – similar shapes of the a priori and the ground-based NO_2 profiles. Thus, the a priori profile shapes calculated with the CTM reproduce the tropospheric NO_2 distribution seen from the ground-based measurements well for clear sky cases. This can also be seen in the scatter plot between VTC_{ind} and $VTC_{\mathrm{ind\_AK}}$ (Fig. 6). Although the latter is slightly higher, the relatively small difference between the two columns can be attributed to the small difference in the two NO_2 profile shapes (it will be shown that this difference is much larger for cloudy cases). Martin et al. (2004) similarly found a good agreement between CTM NO_2 profiles and profile information from aircraft campaigns, although a different model was used to generate a priori profile shapes for the retrieval.

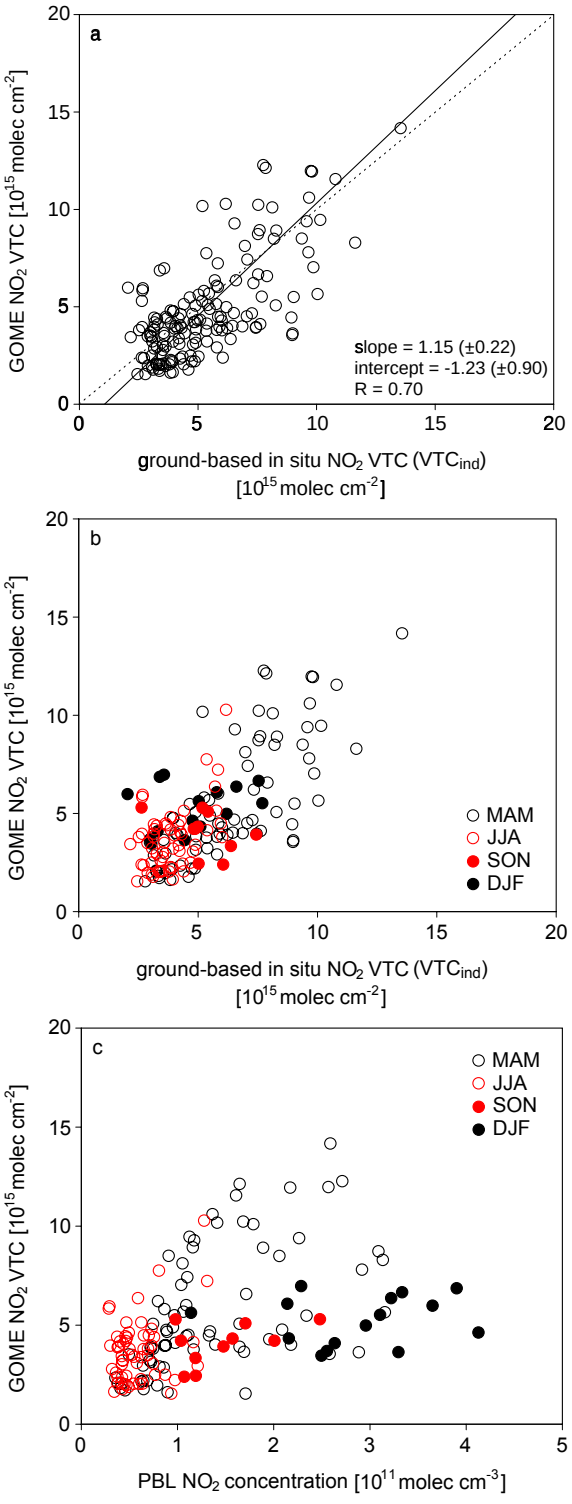

Fig. 4. Clear sky first comparison between GOME NO_2 and the (directly integrated) ground-based NO_2 VTCs including orthogonal regression output **(a)**. The same comparison showing the four seasons MAM, JJA, SON and DJF **(b)**. Qualitative comparison between GOME NO_2 VTCs and PBL NO_2 concentrations **(c)**.

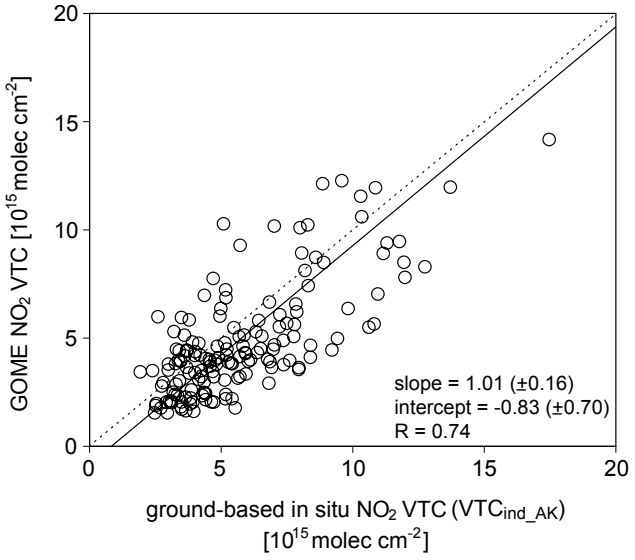

Fig. 5. Clear sky comparisons between GOME NO_2 VTCs and ground-based NO_2 columns with orthogonal regression output for the second comparison (ground-based profiles multiplied with the AK).

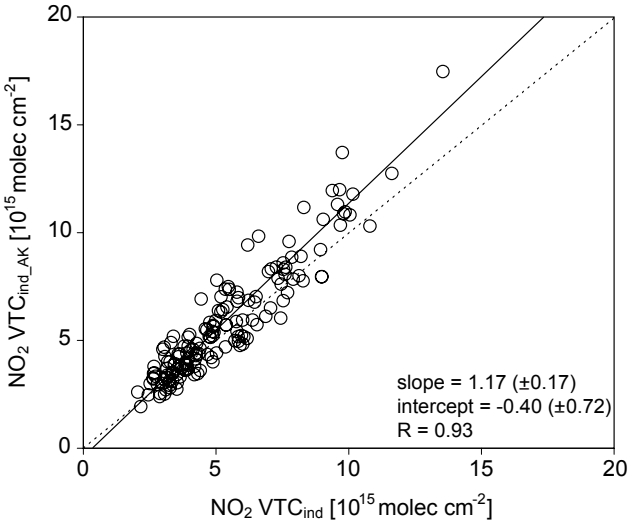

Fig. 6. Clear sky comparison between the directly integrated ground-based NO_2 column (VTC_{ind}) and the corresponding column after multiplication with the AK ($VTC_{\mathrm{ind\_AK}}$). Additionally, the resulting orthogonal regression calculation is shown.

4.3 Quantifying differences between the NO_2 VTCs

In this section, relative differences between the two column data sets are analysed in more detail. The errors in both the GOME and the ground-based NO_2 columns are not taken into account. First, for the whole data set, the mean and median relative difference with respect to the ground-based columns (Δ_0), as well as the mean absolute difference between the columns is compared to results from other studies. This is followed by a detailed analysis of relative differences with respect to the GOME columns (Δ_{1-3}, Sect. 3.2.2).

4.3.1 VTC differences relative to ground-based NO_2 VTCs

For the whole clear sky column data set, the mean, standard deviation and median of Δ_0 are calculated to be -7%, 40% and -13% (Table 4). The standard deviation suggests that the a priori estimates of 50% errors on clear sky GOME and ground-based columns are too conservative, and errors of the order of 30% would be more consistent with the intercomparison results. The mean Δ_0 indicates that on average, the GOME NO_2 VTCs are slightly smaller than the corresponding ground-based columns. This result is consistent with findings from other authors (Table 1) that found GOME columns being smaller than independently measured columns by 14% (Petritoli et al., 2004), 8% (Martin et al., 2004) and 3% (Heland et al., 2001). The mean and median absolute difference between GOME and the directly integrated ground-based columns (VTC_{ind}) are 0.51×10^{15} molec cm^{-2} (with a standard deviation of 1.9×10^{15} molec cm^{-2}) and 0.66×10^{15} molec cm^{-2}, which is comparable to the mean absolute difference of 0.49×10^{15} molec cm^{-2} reported by Martin et al. (2004). Note, however, that there are also considerable differences between the Bremen, Harvard and KNMI/BIRA retrievals (van Noije et al., 2006).

4.3.2 VTC differences relative to GOME NO_2 VTCs: detailed analysis

Unlike Δ_0, Δ_{1-3} are relative differences calculated with respect to the GOME columns. These differences allow splitting the total relative difference (Δ_1) into two contributions,

- Δ_2, which is due to errors in the ground-based NO_2 profile, retrieval errors such as the estimate of the stratospheric background and/or the scattering weights m_l (including estimated forward model parameters such as, e.g., surface albedo),
- Δ_3, which depends on differences between the shapes of the a priori and the ground-based NO_2 profiles.

The mean, standard deviation and median of Δ_{1-3} are calculated for the whole clear sky data set (157 cases) as well as for 3 subclasses equally proportioned: GOME NO_2 VTC<3.5, 3.5–5.0 and $>5.0\times10^{15}$ molec cm^{-2} (Table 4). In the following, we allude to the means, because this allows to write Δ_1 as the sum of Δ_2 and Δ_3.

For the whole clear sky data set, the mean Δ_{1-3} are calculated to be -26%, -34% and 8%, respectively. As Δ_0 before, Δ_1 indicates an underestimation of GOME with respect to the ground-based columns. The mean Δ_2 dominates over Δ_3 with the two contributions compensating each other

Table 4. Mean, standard deviation and median of the relative differences Δ_0 and Δ_{1-3} between GOME and ground-based NO_2 VTCs. Δ_0 is the relative difference calculated with respect to the ground-based columns and is, therefore, comparable to the quantities given in Table 1. Δ_{1-3} are calculated with respect to the GOME columns. This allows to split the total relative difference (Δ_1) into two contributions: one that is due to differences in the shapes of the a priori and the ground-based NO_2 profile (Δ_3), and another that is due to the remaining retrieval parameters and uncertainties in the ground-based profile (Δ_2). For the subclass with GOME NO_2 VTCs$<3.5\times10^{15}$ molec cm^{-2} a second scenario is calculated with ground-based NO_2 columns deduced from ground-based in situ measurements averaged from 06:00–09:00 UTC (instead of 09:00–12:00 UTC).

GOME NO_2 VTC classes ($\times10^{15}$ molec cm^{-2})	n	Δ_0 (%) mean	Δ_0 (%) std. dev.	Δ_0 (%) median	Δ_1 (%) mean	Δ_1 (%) std. dev.	Δ_1 (%) median	Δ_2 (%) mean	Δ_2 (%) std. dev.	Δ_2 (%) median	Δ_3 (%) mean	Δ_3 (%) std. dev.	Δ_3 (%) median
all	157	−7	40	−13	−26	49	−15	−34	48	−27	8	20	9
>5.0	52				7	31	8	−5	35	−4	12	16	13
3.5–5.0	53				−22	44	−14	−30	41	−24	8	23	8
<3.5	52				−61	44	−66	−65	48	−61	4	21	5
<3.5 (06:00–09:00 UTC)	52				−42	45	−38	−49	50	−37	7	19	3

to a certain extent. As Δ_2 is independent of a priori profile errors in the retrieval, the large contribution indicates that the ground-based NO_2 profiles together with the scattering weights are, on average, higher than SCD_{trop}. The small contribution from Δ_3 on the total Δ_1 can be attributed to similar shapes of the a priori and the ground-based NO_2 profiles. This is consistent with the relatively weak impact after inclusion of AK information as discussed in the previous section. The positive value of Δ_3 indicates that the TM4 a priori NO_2 profile shapes are, on average, slightly biased towards higher NO_2 abundances at lower altitudes or smaller NO_2 abundances at higher altitudes. I.e., TM4 profiles tend to peak more towards the surface than the observed profiles.

For the subclass with GOME NO_2 VTCs$>5.0\times10^{15}$ molec cm^{-2}, the mean Δ_{1-3} are calculated to be 7%, −5% and 12%, respectively. Thus, for this data subset, the positive Δ_1 is consistent with GOME columns that are on average exceeding the ground-based columns. This explains the steeper slope for the first comparison (Fig. 4a). The small Δ_2 of −5% indicates that the ground-based NO_2 profiles together with the scattering weights reliably reproduce SCD_{trop}. The remaining Δ_3 of 12% shows that differences in the two NO_2 profile shapes play a major role for this data subset. Therefore, the multiplication of the ground-based profiles with the AK has a larger impact in this data subset and explains to large parts the changing slope between the first and the second comparison (Figs. 4a and 5). The positive value again indicates TM4 a priori NO_2 profile shapes that are, on average, biased towards higher NO_2 abundances at lower altitudes or smaller NO_2 abundances at higher altitudes. The reasons for that are manifold and could be uncertainties in the NO_x emission inventories, uncertainties arising from the CTM, uncertainties in the meteorological fields (e.g. an underestimation of vertical transport in the alpine region), but also errors in the ground-based NO_2 profile. Which of the uncertainties is dominant is not clear.

For the subclasses with GOME NO_2 VTCs between 3.5 and 5.0×10^{15} molec cm^{-2} and $<3.5\times10^{15}$ molec cm^{-2}, Δ_{1-3} are calculated to be −22%, −30% and 8% and −61%, −65% and 4%, respectively (Table 4). Thus, for lower GOME NO_2 column values,

- Δ_1 is increasing with GOME columns underestimating the ground-based columns,
- Δ_2 is increasing as well, indicating that SCD_{trop} underestimates the slant column given by the ground-based profile together with the scattering weights,
- the profile shapes are more similar than for situations with high GOME NO_2 column values.

The increasing Δ_1 towards smaller GOME columns is mainly explained by Δ_2. This is the main reason for the offsets found in the orthogonal regression calculations (Figs. 4a and 5). Therefore, Δ_1 can no longer be explained by different NO_2 profile shapes, but by uncertainties in the ground-based NO_2 profiles, retrieval errors such as the estimate of the stratospheric background and/or the scattering weights.

Smaller NO_2 columns in both data sets often occur in the summer season (Fig. 4b). Therefore, one might argue that the increase in Δ_2 towards smaller columns is mainly due to thermal upslope transport of NO_2 that leads to a systematic overestimation of the NO_2 located at elevated levels in the ground-based profiles. To check this, we changed the averaging time window (for calculating the average NO_2 concentration for the ground stations; see Sect. 3.1.1) from 09:00–12:00 to 06:00–09:00 UTC. For this time window, the influence from thermal upslope transport at the elevated stations can be expected to be small. For GOME NO_2 VTCs$<3.5\times10^{15}$ molec cm^{-2} the resulting Δ_{1-3} are −42%, −49% and 7%, respectively (Table 4). Although Δ_1 and Δ_2 now indicate a smaller relative difference between the column data sets, thermal upslope transport of pollution only explains 1/3 (1/2 if the median is considered) of the relative

difference. It therefore seems likely that, towards smaller NO_2 columns, GOME retrievals over the study area indeed underestimate the true NO_2 column. This would be consistent with some unrealistically small GOME NO_2 VTCs that have been found (and that have been excluded from the comparison by the criterion SCD_{trop}/SCD, as pointed out at the beginning of Sect. 4.2). For instance, the smallest clear sky GOME column of 0.05×10^{15} molec cm^{-2} was detected over an area covering the most polluted part of the Swiss Plateau including the largest Swiss cities Zurich and Basel. The total and the stratospheric SCD are very similar in this case (7.74×10^{15} molec cm^{-2} and 7.71×10^{15} molec cm^{-2}, respectively), and uncertainty in the latter can at least partially explain the small GOME NO_2 VTC value.

The investigation described above should be refined further in the future. Particularly for cases with Δ_2 explaining the major part of Δ_1, independent knowledge of non-profile retrieval parameters, such as surface albedo, would shed further light on the reason for column differences. The results presented here should be seen as tendencies, because averaged differences with large standard deviations are discussed. This means that for single day-to-day cases, parameters such as the a priori NO_2 profile shape can have a much larger (but also lower) impact than averaged over the whole data set. Moreover, the investigated GOME pixels exhibit a large extension always detecting a somewhat changing mix of remote and polluted areas in the study area. For future work with smaller pixels from SCIAMACHY (60×30 km^2) or the Ozone Monitoring Instrument (OMI, 13×24 km^2), the pixel-to-pixel NO_2 VTC differences can be expected to be much larger with remote and polluted pixels lying close to each other and probably being retrieved with similar or even the same a priori profile shapes (due to significant spatial undersampling with coarser resolved CTMs). We would therefore expect that the tendencies found in the present study will come out clearer for satellite pixels with a lower extension.

5 Results for cloudy conditions

A detailed comparison for cloudy GOME pixels has so far not been carried out. The potential retrieval errors under cloudy conditions can, however, be thought to be much larger than for clear sky conditions. This is mainly due to inaccurate knowledge of cloud characteristics (e.g. cloud top height, cloud fraction, optical thickness) and difficulties in the radiative transfer modelling (multiple scattering). For the comparison under cloudy conditions the following has to be fulfilled:

- GOME pixel location above northern Switzerland (Fig. 1),
- GOME pixel cloud fraction from FRESCO (Koelemeijer et al., 2001) $\geq$0.75,
- SCD_{trop}/SCD$>$10%.

Figure 7a shows the first and the second comparison between the GOME and the ground-based NO_2 VTCs for 76 cloudy cases. Obviously, there are a number of cases with a very poor agreement, with GOME columns being up to a factor of 20 higher than the ground-based columns. The reason for the strong disagreement for these cases is discussed qualitatively at the example of the most extreme case on 17 February 2001.

Based on GOME NO_2 measurements, Schaub et al. (2005) have shown that, during 16 and 17 February 2001, frontal activity over Central Europe caused vertical transport of polluted near-ground air masses to up to approximately 4000 m a.s.l. No lightning activity was detected during that episode (http://www.wetterzentrale.de/topkarten/tkbeoblar.htm), but the vertical transport led to a significant amount of NO_2 being located within and above a dense cloud cover with a top height of approximately 700 hPa. Because of the high sensitivity of the space-borne instrument above reflecting clouds, this is consistent with a large SCD_{trop} of 57×10^{15} molec cm^{-2} (which is nearly 90% of the total SCD of 64×10^{15} molec cm^{-2}) given by the KNMI/BIRA data set. From this, an unrealistically high GOME NO_2 VTC value of 489.5×10^{15} molec cm^{-2} is retrieved.

The corresponding ground-based NO_2 VTCs are calculated to be 22.4×10^{15} molec cm^{-2} (directly integrated) and 38.3×10^{15} molec cm^{-2} (AK included). The strong disagreement between the latter and the GOME column indicates that the ground-based profile together with the scattering weights is much smaller than SCD_{trop}. Thus, two main reasons could explain the strong disagreement: on the one hand, the scattering weights could be wrong due to errors in the radiative transfer modelling resulting from uncertainties in the cloud parameters. It has been mentioned in Sect. 2.1 that errors induced by uncertainties in the cloud top height are increasing for situations with enhanced NO_2 concentrations close to the cloud top height (which is the case here). On the other hand, the disagreement can just as well be attributed to the ground-based profile: first, no NO_2 measurements from the high-alpine site Jungfraujoch are available for this episode (such data gaps can be neglected when calculating a clear sky column with typically very low NO_2 concentrations at Jungfraujoch; however, they become important when polluted air masses reach the station and the latter additionally being located above a reflecting cloud cover). Second, the peak NO_2 concentrations measured at the ground stations occurred rather in the evening of the 17 February, and not during the time of the GOME overpass. This shows that the assumption of a homogeneous NO_2 distribution at elevated levels may not be valid for this case.

Therefore, a new scenario is calculated based on the following assumptions: a) the Jungfraujoch station measures the same NO_2 concentration as the Zugspitze station, and b) every ground station contributes to the ground-based column with its maximum NO_2 concentration measured during the frontal passage (i.e. during 17 and the first

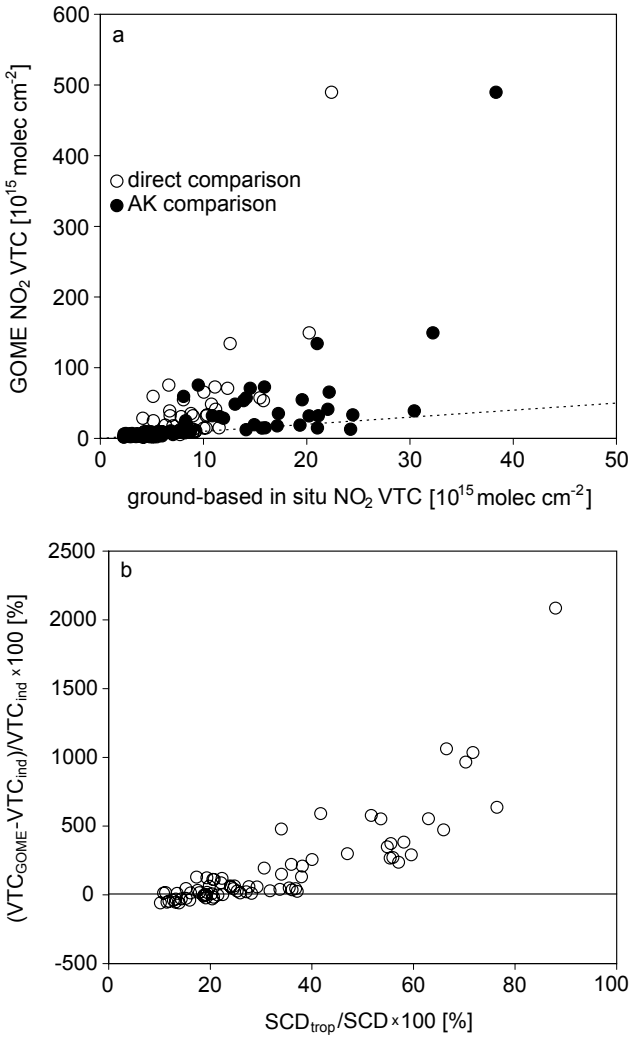

Fig. 7. First and second comparison for cloudy conditions (note the unrealistically high columns that can be retrieved under such conditions) **(a)**. Relative difference (Δ_0) between GOME and ground-based NO_2 VTCs (VTC_{ind}) as a function of fraction of SCD_{trop} on the total SCD **(b)**.

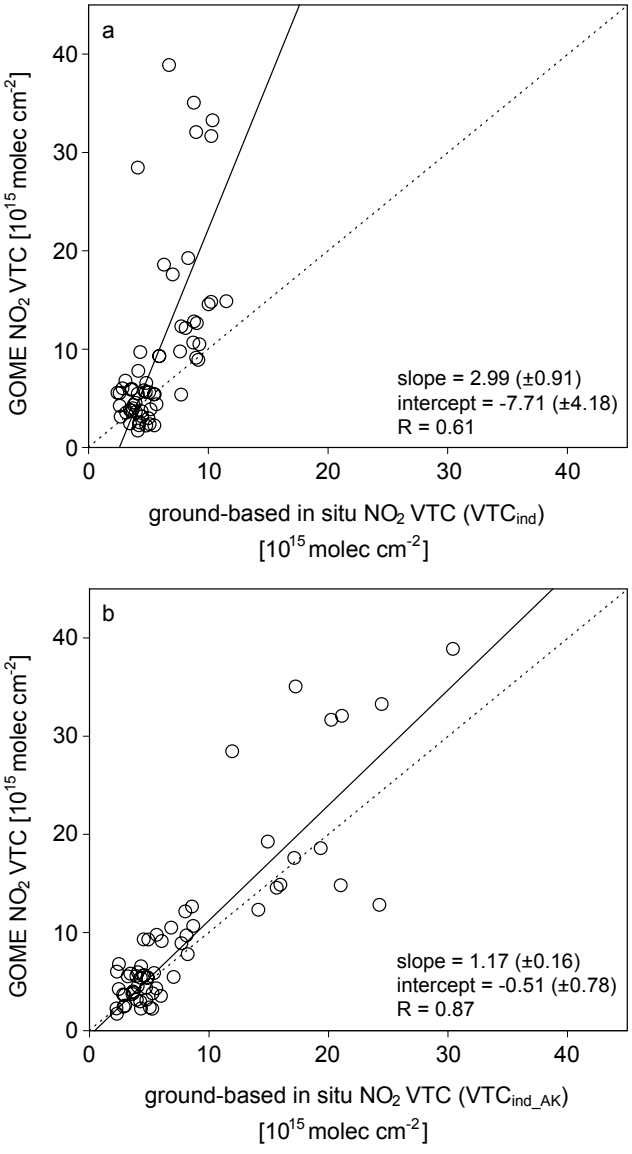

Fig. 8. First comparison between GOME NO_2 VTCs and tropospheric columns derived from ground-based in situ measurements **(a)** and second comparison after multiplying the ground-based profile with the averaging kernel **(b)** together with orthogonal regression output for cloudy conditions. Columns with SCD_{trop}/SCD>50% are rejected.

half of 18 February). This yields ground-based columns of 46.7×10^{15} molec cm^{-2} (directly integrated, VTC_{ind}) and 304.8×10^{15} molec cm^{-2} after multiplication with the AK ($VTC_{\mathrm{ind\_AK}}$).

VTC_{ind} still strongly underestimates the GOME NO_2 VTC, although the lower ground stations contributed with high concentrations in the order of 30 ppb to the column. Remarkably, for this new scenario, $VTC_{\mathrm{ind\_AK}}$ results in a value that is at least of the same order as the GOME column of 489.5×10^{15} molec cm^{-2}. The distinct change in the ground-based columns after multiplication with the AK indicates that the shapes of the ground-based and the a priori NO_2 profile are strongly differing. The increase of the column after multiplication with the AK is consistent with a TM4 a priori NO_2 profile shape that is biased towards higher NO_2 abundances at lower altitudes or smaller NO_2 abundances at higher altitudes. The latter point gives evidence for the following additional explanation of the large GOME column during this episode (besides uncertain cloud parameters): the frontal transport event results in complex air mass mixing together with horizontal and vertical movement which may not be properly reproduced by the coarsely resolved global CTM. The CTM might therefore calculate an a priori NO_2 profile that underestimates the enhanced NO_2

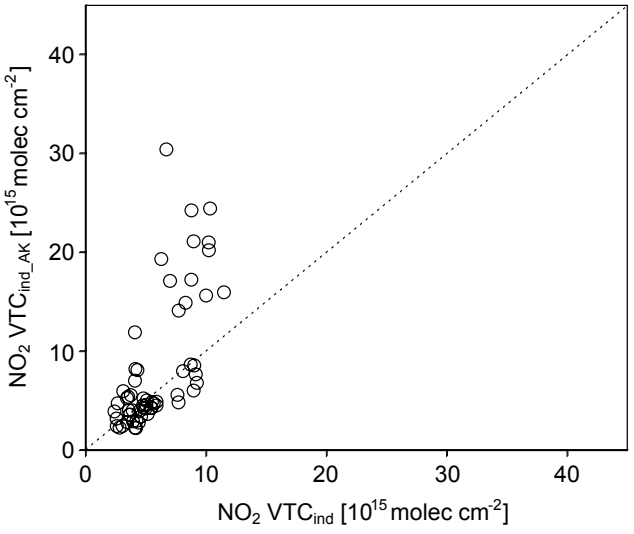

Fig. 9. Directly integrated ground-based NO_2 column (VTC_{ind}) and the corresponding column multiplied with the AK ($VTC_{\mathrm{ind\_AK}}$) for cloudy conditions.

amount within and above the clouds. This further leads to an underestimation of the AMF_{trop}. The latter, together with the very high SCD_{trop} value, results in a strong overestimation of the NO_2 VTC. The AK convoluted surface measurement, however, shows a reasonable agreement with the GOME retrieval. This indicates the GOME measurement to be consistent within error bars with the ground-based column amount for this special case.

It becomes obvious from Fig. 7a, that there are other cases with very high GOME NO_2 VTC values that, also after multiplication with the AK, do not agree with the ground-based columns. These cases are similar to the case from 17 February 2001 described above. Figure 7b shows that the Δ_0 between the GOME NO_2 VTCs and the corresponding ground-based columns are increasing for increasing SCD_{trop}/SCD ratios. This indicates that (frontal) transport events that lead to NO_2 pollution at elevated levels, and thus high SCD_{trop} values, are difficult to handle for both the retrieval but also for the comparison with ground-based NO_2 profiles (due to representativity errors in the latter).

For the further investigation, the most extreme cases with SCD_{trop}/SCD>50% are rejected from the data set. This SCD_{trop}/SCD criterion is chosen arbitrarily. For the first comparison of the remaining 60 cases (Fig. 8a), the orthogonal regression calculates a slope of 2.99 ($\pm$0.91), an intercept of -7.71 ($\pm$4.18) and a correlation coefficient R=0.61. In consistency with a mean Δ_0 of 60% (with a standard deviation of 118%) this indicates GOME columns on average clearly overestimating the ground-based columns. The second comparison leads to a much better agreement for the average of the cloudy cases (Fig. 8b) with slope, intercept and correlation coefficient changing to 1.17 ($\pm$0.16), -0.51 ($\pm$0.78) and R=0.87, respectively. Thus, differences between the two NO_2 profile shapes play a more important role under cloudy conditions. This is further supported by mean Δ_{1-3} that are calculated to be 10%, 3% and 7%, respectively, with Δ_3 explaining the major part of the total relative difference. Moreover, this is mirrored in a poorer agreement between VTC_{ind} and $VTC_{\mathrm{ind\_AK}}$ (Fig. 9) than found for the clear sky cases (Fig. 6). This supports the conclusion that for the average of the cloudy cases, the retrieval error due to uncertainties in the a priori profile shapes becomes more important. As pointed out in the above case example, a positive value for Δ_3 would be consistent with an underestimation of upward transport of NO_2 in the CTM. As a consequence, the AMF_{trop} would be under- and the corresponding GOME NO_2 VTCs overestimated.

Note that the clear improvement after multiplication with the AK can also be found for other choices of the above rejection criterion SCD_{trop}/SCD (not shown). Only towards low SCD_{trop}/SCD values, the impact of AK is decreasing and comparable to the impact found for the clear sky cases. This becomes obvious from Fig. 8, where the comparison with larger GOME NO_2 columns is stronger affected by the multiplication with the AK than the comparison with smaller columns. If the impact of AK information is taken as a measure for the uncertainty of a priori NO_2 profiles (and the resulting GOME NO_2 columns) under cloudy conditions, we qualitatively estimate from Fig. 8, that for the study region, already GOME columns exceeding 10×10^{15} molec cm^{-2} should be handled with care before being further used for air pollution monitoring or as input parameters for models. Or in other words: for such cases, the proper use of averaging kernel information is a matter of special importance and the absolute value of the retrieval should be interpreted carefully.

6 Summary and conclusions

A long-term comparison of GOME NO_2 VTC data retrieved from KNMI/BIRA with independently derived NO_2 columns was carried out. The study compared GOME NO_2 VTCs over Northern Switzerland with coincident ground-based tropospheric columns for both anticyclonic clear sky (GOME pixel cloud fraction $\leq$0.1) and cloudy conditions (cloud fraction $\geq$0.75).

Ground-based in situ NO_2 profiles/columns were deduced from ground stations located at different altitudes in the Alps and Swiss Plateau (PBL) stations representative for different pollution levels. An error estimate for these ground-based NO_2 columns took into account the non-selective NO_2 measurements with molybdenum converters and inhomogeneities at stations located at around 1000 m a.s.l. (e.g. due to thermal transport). The resulting error in the ground-based columns is in the order of 50%, which is comparable to the 1-sigma errors estimated for the GOME NO_2 VTCs.

A first comparison related the GOME columns to the ground-based NO_2 profiles that are directly integrated to tropospheric columns. For a second comparison, the ground-based profiles are multiplied with the averaging kernel (AK). This makes the comparison independent from the a priori NO_2 profile used in the GOME retrieval. Thus, the total relative difference between the column data sets can be split into two contributions: one that depends on the differences between the a priori and the ground-based NO_2 profile shapes, and another which is no longer affected by the a priori NO_2 profile, but depends on errors in both the remaining retrieval parameters and the ground-based NO_2 profiles.

The clear sky comparison (157 cases) showed a good agreement between the two columns types. The seasonal behaviour is very similar, with smallest NO_2 VTCs during summertime and largest columns in the spring season. An orthogonal regression taking into account error estimates for both column types yielded a slope and an intercept of 1.15 (std. dev. 0.22) and -1.23 (std. dev. 0.90), respectively, with a correlation coefficient R=0.70. After AK inclusion, the slope and intercept changed to 1.01 (std. dev. 0.16) and -0.83 (std. dev. 0.70), respectively, with R=0.74. The multiplication of the ground-based profile with the AK has a relatively weak impact. This can be attributed to similar shapes of the ground-based and the a priori NO_2 profile for the average of the anticyclonic clear sky cases.

A detailed analysis of relative differences between the two data sets was carried out. For the whole clear sky data set a mean relative difference (with respect to the ground-based columns) of -7% with a standard deviation of 40% is found, with GOME NO_2 VTCs slightly underestimating the ground-based columns. The standard deviation result suggests that the a priori estimates of 50% errors on GOME and ground-based columns are too conservative, and errors of the order of 30% would be more consistent with the intercomparison results.

The further analysis showed that the above mentioned contributions to the total relative compensate each other to a certain extent for clear sky cases. This should be taken into account in detailed validation studies of space-borne data that are affected by uncertainties in a number of parameters. Further, the following evidences were found (with relative differences calculated with respect to the GOME columns):

- For large GOME NO_2 VTCs ($>5.0\times10^{15}$ molec cm^{-2}), the GOME product is slightly larger (7%) than the ground-based columns. This is mainly caused by differences between the ground-based and the a priori NO_2 profile shapes.
- For smaller GOME NO_2 VTCs (<3.5 and 3.5–5.0×10^{15} molec cm^{-2}), the GOME product is smaller than the ground-based one (with a mean relative difference of up to -61%) due to other error sources than the a priori NO_2 profile assumptions (i.e., remaining retrieval parameters and/or ground-based NO_2 profiles).

The comparison for cloudy conditions generally yielded a poorer agreement between the columns. This can be expected due to additional error sources arising from inaccurate knowledge of cloud characteristics (e.g. cloud top height, cloud fraction, optical thickness) and difficulties in the radiative transfer modelling (multiple scattering). Unrealistically large GOME NO_2 VTCs have been found, e.g. for 17 February 2001, with a tropospheric GOME column of 490×10^{15} molec cm^{-2}. Evidences are discussed that such high column values are likely due to an underestimation of the elevated NO_2 in the a priori profile in combination with retrieval errors due to inaccurate cloud parameters which lead to a strong magnification of above-cloud NO_2 concentrations. Also after excluding extremely large GOME columns, the remaining GOME NO_2 VTCs (60 cases) still overestimate the ground-based columns. The mean relative difference (with respect to the ground-based columns) is 60% with a standard deviation of 118%.

For the first comparison, the orthogonal regression yielded a slope and an intercept of 2.99 (std. dev. 0.91) and -7.71 (std. dev. 4.18), respectively, with a correlation coefficient R=0.61. For the second comparison, the slope and intercept changed to 1.17 (std. dev. 0.16) and -0.51 (std. dev. 0.78), respectively, with R=0.87. The multiplication with the AK clearly improved the comparison. This is consistent with a larger difference between the ground-based and the a priori NO_2 profile shapes and gives evidence for uncertainties in the a priori NO_2 profiles playing a more important role for the retrieval of cloudy scenes than for clear sky cases. This mainly applies for high GOME NO_2 column values ($>10\times10^{15}$ molec cm^{-2} for the study area). Therefore the inclusion of averaging kernel information is crucial for use of such retrievals, and the absolute value of the retrieval should be interpreted carefully in this case.

The good agreement between GOME and ground-based NO_2 VTCs found in the present study for clear sky conditions encourages the use of space-borne trace gas columns for air pollution modelling and monitoring also on a regional scale. The good agreement is remarkable taking into account both the complex topography at the foothills of the Alps and the uncertainties in both column data sets. The study further showed that comparison or validation studies of space-borne trace gas columns with independently derived profiles should include averaging kernel information in order to distinguish between different error sources. We expect this to become even more important for future comparisons with higher resolved pixels from SCIAMACHY and OMI (particularly with regard to a possible undersampling when calculating a priori NO_2 profiles with coarsely resolved global CTMs). However, this is a first step towards a more detailed comparison. A further improvement of comparison or validation studies can be reached by including independent knowledge of retrieval parameters such as surface albedo, satellite pixel surface pressure, and, for comparisons under cloudy conditions, cloud parameters. Moreover, the present study

investigated absolutely cloud-free (GOME pixel cloud fraction $\leq$0.1) and clearly cloudy scenes (cloud fraction $\geq$0.75). Hence, work remains to be done on retrievals in situations of moderate cloudiness.

Acknowledgements. This work was funded by the Swiss Federal Office for the Environment (FOEN) and the Swiss Federal Laboratories for Materials Testing and Research (Empa). For providing ground-based in situ measurements we acknowledge the Swiss National Air Pollution Monitoring Network (NABEL), the Federal Environmental Agency (FEA, Germany), the German Weather Service (DWD), the Zentrum für Umweltmessungen, Umwelterhebungen und Gerätesicherheit Baden-Württemberg (UMEG) and the Bavarian Environmental Protection Agency (LFU). We thank I. DeSmedt and M. Van Roozendael (BIRA/IASB) and R. van der A (KNMI) for their work on making available the TEMIS GOME NO_2 data set used in this study.

Edited by: R. Volkamer

References

Beyrich, F., Gryning, S.-E., Joffre, S., Rasmussen, A., Seibert, P., and Tercier, P.: Mixing height determination for dispersion modelling – a test of meteorological pre-processors, Air Pollution Modeling and Its Application, Plenum Press, New York, 1998.

Boersma, K. F., Eskes, H. J., and Brinksma, E. J.: Error analysis for tropospheric NO_2 retrieval from space, J. Geophys. Res., 109, art. no. 4311, doi:10.1029/2003JD003962, 2004.

Boersma, K. F., Eskes, H. J., Meijer, W., and Kelder, H. M.: Estimates of lightning NO_x production from GOME satellite observations, Atmos. Chem. Phys., 5, 2311–2221, 2005, http://www.atmos-chem-phys.net/5/2311/2005/.

Bovensmann, H., Burrows, J. P., Buchwitz, M., Frerick, J., Noël, S., and Rozanov, V. V.: SCIAMACHY: Mission objectives and measurement modes, J. Atmos. Sci., 56(2), 127–150, 1999.

Brasseur, G. P.: Atmospheric chemistry in a changing world, Springer Verlag, Berlin, 2003.

Burrows, J. P., Weber, M., Buchwitz, M., Rozanov, V., Ladstätter-Weissenmayer, A., Richter, A., DeBeek, R., Hoogen, R., Bramstedt, K., Eichmann, K. U., Eisinger, M., and Perner, D.: The global ozone monitoring experiment (GOME): Mission concept and first scientific results, J. Atmos. Sci., 56, 151–175, 1999.

BUWAL: NABEL – Luftbelastung 2003, Schriftenreihe Umwelt Nr. 370, 2004.

Choi, Y., Wang, Y., Zeng, T., Martin, R. V., Kurosu, T. P., and Chance, K.: Evidence of lightning NO_x and convective transport of pollutants in satellite observations over North America, Geophys. Res. Lett., 32, L02805, doi:10.1029/2004GL021436, 2005.

Clemitshaw, K. C.: A review of instrumentation and measurement techniques for ground-based and airborne field studies of gas-phase chemistry, Crit. Rev. in Env. Sc. and Techn., 34, 1–108, 2004.

Dentener, F. J. and Crutzen, P. J.: Reaction of N_2O_5 on tropospheric aerosols: impact on the global distributions of NO_x, O_3 and OH, J. Geophys. Res., 98, 7149–7163, 1993.

Dentener, F. J., van Weele, M., Krol, M., Houweling, S., and van Velthoven, P.: Trends and inter-annual variability of methane emissions derived from 1979–1993 global CTM simulations, Atmos. Chem. Phys., 3, 73–88, 2003, http://www.atmos-chem-phys.net/3/73/2003/.

Empa: Technischer Bericht zum Nationalen Beobachtungsnetz für Luftfremdstoffe (NABEL), Duebendorf, 2005.

Eskes, H. J. and Boersma, K. F.: Averaging kernels for DOAS total-column satellite retrievals, Atmos. Chem. Phys., 3, 1285–1291, 2003, http://www.atmos-chem-phys.net/3/1285/2003/.

Eskes, H. J.: Combined retrieval, modeling and assimilation approach to GOME NO_2, in GOA final report, European Commission 5th framework programme 1998–2002, EESD-ENV-99-2, 116–122, Eur. Comm., De Bilt, Netherlands, 2003.

Finlayson-Pitts, B. J. and Pitts, J. N.: Chemistry of the upper and lower Atmosphere – Theory, Experiments and Applications, Academic Press, San Diego, CA, 2000.

Forrer, J., Rüttimann, R., Schneiter, D., Fischer, A., Buchmann, B., and Hofer, P.: Variability of trace gases at the high-Alpine site Jungfraujoch caused by meteorological transport processes, J. Geophys. Res., 105, 12 241–12 251, 2000.

Heland, J., Schlager, H., Richter, A., and Burrows, J. P.: First comparison of tropospheric NO_2 column densities retrieved from GOME measurements and in situ aircraft profile measurements, Geophys. Res. Lett., 29, 1983, doi:10.1029/2002GL015528, 2002.

Herwehe, J. A., McNider, R. T., and Newchurch, M. J.: A numerical study of the effects of large eddies photochemistry in the convective boundary layer, Reprint from the American Meteorological Society's 14th Symposium on Boundary Layer and Turbulence, Aspen, CO, 2000.

Heue, K.-P., Richter, A., Bruns, M., Burrows, J. P., v. Friedeburg, C., Platt, U., Pundt, I., Wang, P., and Wagner, T.: Validation of SCIAMCHY tropospheric NO_2-columns with AMAXDOAS measurements, Atmos. Chem. Phys., 5, 1039–1051, 2005, http://www.atmos-chem-phys.net/5/1039/2005/.

Holtslag, A. A. M., De Bruin, E. I. F., and Pan, H.-L.: A high resolution air mass transformation model for short range weather forecasting, Monthly Weather Rev., 118, 1561–1575, 1990.

Horowitz, L. W., Walters, S., Mauzerall, D. L., Emmons, L. K., Rasch, P. J., Granier, C., Tie, X. X., Lamarque, J. F., Schultz, M. G., Tyndall, G. S., Orlando, J. J., and Brasseur, G. P.: A global simulation of tropospheric ozone and related tracers: Description and evaluation of MOZART, version 2, J. Geophys. Res., 108, 4784, doi:10.1029/2002JD002853, 2003.

Jaeglé, L., Jacob, D. J., Wang, Y., Weinheimer, A. J., Ridley, B. A., Campos, T. L., Sachse, G. W., and Hagen, D. E.: Sources and chemistry of NO_x in the upper troposphere over the United States, Geophys. Res. Lett., 25, 1705–1708, 1998.

Koelemeijer, R. B. A., Stammes, P., Hovenier, J. W., and de Hann, J. F.: A fast method for retrieval of cloud parameters using oxygen A-band measurements from Global Ozone Monitoring Experiment, J. Geophys. Res., 106, 3475–3490, 2001.

Kramm, G., Dlugi, R., Dollard, G. J., Foken, T., Mölders, N., Müller, H., Seiler, W., and Sievering, H.: On the dry deposition of ozone and reactive nitrogen species, Atmos. Environ., 29, 3209–3231, 1995.

Lugauer, M., Baltensperger, U., Furger, M., Gäggeler, H. W., Jost, D. T., Schwikowski, M., and Wanner, H.: Aerosol transport to the high Alpine sites Jungfraujoch (3454 m asl) and Colle Gnifetti

(4452 m asl), Tellus, 50B, 76–92, 1998.

Lugauer, M., Baltensperger, U., Furger, M., Gäggeler, H. W., Jost, D. T., Nyeki, S., and Schwikowski, M.: Influences of vertical transport and scavenging on aerosol particle surface area and radon decay product concentrations at the Jungfraujoch (3454 m asl), J. Geophys. Res., 105, 19 869–19 879, 2000.

Martin, R. V., Parrish, D. D., Ryerson, T. B., Nicks, D. K., Chance, K., Kurosu, T. P., Jacob, D. J., Sturges, E. D., Fried, A., and Wert, B. P.: Evaluation of GOME satellite measurements of tropospheric NO_2 and HCHO using regional data from aircraft campaigns in the southeastern United States, J. Geophys. Res., 109, D24307, doi:10.1029/2004JD004869, 2004.

MeteoSwiss: Alpine Weather Statistics (Alpenwetterstatistik – Witterungskalender: Beschreibung der einzelnen Parameter), MeteoSwiss, Switzerland, 1985.

Moxim, W. J., Levy II, H., and Kasibhatla, P. S.: Simulated global tropospheric PAN: Its transport and impact on NO_x, J. Geophys. Res., 101, 12 621–12 638, 1996.

Navas, M. J., Jiménez, A. M., and Galan, G.: Air analysis: determination of nitrogen compounds by chemiluminescence, Atmos. Environ., 31, 3603–3608, 1997.

Nyeki, S., Kalberer, M., Colbeck, I., De Wekker, S., Furger, M., Gäggeler, H. W., Kossmann, M., Lugauer, M., Steyn, D., Weingartner, E., Wirth, M., and Baltensperger, U.: Convective boundary layer evolution to 4 km asl over high-alpine terrain: airborne lidar observations in the Alps, Geophys. Res. Lett., 27, 689–692, 2000.

Ordóñez, C., Richter, A., Steinbacher, M., Zellweger, C., Nüss, H., Burrows, J. P., and Prévôt, A. S. H.: Comparison of 7 years of satellite-borne and ground-based tropospheric NO_2 measurements around Milan, Italy, J. Geophys. Res., 111(D5), D05310, doi:10.1029/2005JD006305, 2006.

Palmer, P. I., Jacob, D. J., Chance, K., Martin, R. V., Spurr, R. J. D., Kurosu, T. P., Bey, I., Yantosca, R., Fiore, A., and Li, Q.: Air mass factor formulation for spectroscopic measurements from satellites: Application to formaldehyde retrievals from the Global Ozone Monitoring Experiment, J. Geophys. Res., 106, 14 539–14 550, 2001.

Penkett, S. A. and Brice, K. A.: The spring maximum in the photooxidants in the northern-hemisphere troposphere, Nature, 319, 655–657, 1986.

Petritoli, A., Bonasoni, P, Giovanelli, G., Ravegnani, F., Kostadinov, I., Bortoli, D., Weiss, A., Schaub, D., Richter, A., and Fortezza, F.: First comparison between ground-based and satellite-borne measurements of tropospheric nitrogen dioxide in the Po basin, J. Geophys. Res., 109, D15307, doi:10.1029/2004JD004547, 2004.

Pisano, J. T., McKendry, I., Steyn, D. G., and Hastie, D. R.: Vertical nitrogen dioxide and ozone concentrations measured from a tethered balloon in the lower Fraser valley, Atmos. Environ., 31, 2071–2078, 1997.

Ridley, B. A., Walega, J. G., Lamarque, J.-F., Grahek, F. E., Trainer, M., Hübler, G., Lin, X., and Fehsenfeld, F. C.: Measurements of reactive nitrogen and ozone to 5-km altitude in June 1990 over the southeastern United States, J. Geophys. Res., 103, 8369–8388, 1998.

Rodgers, C. D.: Inverse methods for atmospheric sounding: theory and practice, Ser. Atmos. Oceanic Planet. Phys., World Scientific Publishing, Singapore, 2000.

Schaub, D., Weiss, A. K., Kaiser, J. W., Petritoli, A., Richter, A., Buchmann, B., and Burrows, J. P.: A transboundary transport episode of nitrogen dioxide as observed from GOME and its impact in the Alpine region, Atmos. Chem. Phys., 5, 23–37, 2005, http://www.atmos-chem-phys.net/5/23/2005/.

Seibert, P., Beyrich, F., Gryning, S.-E., Joffre, S., Rasmussen, A., and Tercier, P.: Review and intercomparison of operational methods for the determination of the mixing height, Atmos. Environ., 34, 1001–1027, 2000.

Seinfeld, J. H. and Pandis, S. N.: Atmospheric chemistry and physics – from air pollution to climate change, John Wiley & Sons, New York, 1998.

Solomon, S., Portmann, W., Sanders, R. W., Daniel, J. S., Madsen, W., Bartram, B., and Dutton, E. G.: On the role of nitrogen dioxide in the absorption of solar radiation, J. Geophys. Res., 104, 12 047–12 058, 1999.

Spicer, C. W.: Nitrogen oxide reactions in the urban plume of Boston, Science, 215, 4536, 1095–1097, 1982.

Staehelin, J., Prévôt, A. S. H., and Barnes, I.: Photochemie der Troposphäre, in: Handbuch der Umweltveränderungen und Oekotoxikologie – Atmosphäre, edited by: Guderian, R., Springer Verlag, Berlin, 2000.

Stammes, P.: Spectral radiance modelling in the UV-Visible Range, in: IRS 2000: Current problems in Atmospheric Radiation, edited by: Smith, W. L. and Timofeyev, Y. M., A. Deepak Publ., Hampton (VA), 2001.

Troen, I. and Mahrt, L.: A simple model of the planetary boundary layer: Sensitivity to surface evaporation, Boundary-Layer Meteor., 37, 129–148, 1986.

Umweltbundesamt: Jahresbericht 2002 aus dem Messnetz des Umweltbundesamtes, 69, Berlin, 2003.

Van Noije, T. P. C., Eskes, H. J., Dentener, F. J., et al.: Multimodel ensemble simulations of tropospheric NO_2 compared with GOME retrievals for the year 2000, Atmos. Chem. Phys., 6, 2943–2979, 2006, http://www.atmos-chem-phys.net/6/2943/2006/.

Vandaele, A. C., Fayt, C., Hendrick, F., et al.: An intercomparison campaign of ground-based UV-visible measurements of NO_2, BrO, and OClO slant columns: Methods of analysis and results for NO_2, J. Geophys. Res., 110, D08305, doi:10.1029/2004JD005423, 2005.

Vogelezang, D. H. P. and Holtslag, A. A. M.: Evaluation and model impacts of alternative boundary-layer height formulations, Boundary-Layer Meteor., 81, 245–269, 1996.

Warneck, P.: Chemistry of the natural atmosphere, second edition, Academic Press, London, 2000.

York, D.: Least-square fitting of a straight line, Can. J. Phys., 44, 1079–1086, 1966.

Zellweger, C., Forrer, J., Hofer, P., Nyeki, S., Schwarzenbach, B., Weingartner, E., Ammann, M., and Baltensperger U.: Partitioning of reactive nitrogen (NO_y) and dependence on meteorological conditions in the lower free troposphere, Atmos. Chem. Phys., 3, 779–796, 2003, http://www.atmos-chem-phys.net/3/779/2003/.